

## COMPOSITE NANOFIBERS OF ELECTROACTIVE POLYMERS PREPARED VIA ELECTROSPINNING

N.J. Pinto<sup>1,\*</sup>, W. Serrano<sup>1</sup>

<sup>1</sup>*Department of Physics and Electronics, University of Puerto Rico – Humacao, Humacao PR 00792*  
*\*nicholas.pinto@upr.edu*

**Keywords:** PVDF-TrFE, PEDOT, Nanofibers, Electrospinning

### Abstract

*Sub-30nm diameter nanofibers of PVDF-TrFE/PEDOT were fabricated using electrospinning. PEDOT assisted in the fabrication of ferroelectric PVDF-TrFE nanofibers at low concentrations in DMF. The composite fibers were conducting and used to fabricate a Schottky diode that was analyzed using the standard thermionic emission model of a Schottky junction.*

### 1 Introduction

Polymeric materials are commonly used in packaging due to their compressibility and light weight. Some polymers, in addition to possessing the above features, can be made electronically functional via introducing free charge into the polymer backbone (conducting polymers)[1,2] or via electric field orientation of the bound charge along the polymer backbone (ferroelectric polymers)[3-5]. The discovery of such conducting and ferroelectric polymers has subsequently led to new advances in flexible electronic devices at reduced cost. Poly(3,4-ethylenedioxythiophene) doped with poly styrene sulfonic acid (PEDOT-PSSA) is a commercially available conducting polymer that is frequently used in plastic electronics primarily as interconnects, while poly(vinylidene fluoride-trifluoroethylene) (PVDF-TrFE) in the ratio 75:25 is a common ferroelectric polymer used in memory chips[6,7]. Much research in this area has centered on the study of each of these polymers *individually* with few reports on their composites[8,9]. Further, the research is mostly on thin films with limited published reports on nanofibers of these composite polymers. The fabrication of true nanofibers ( $d < 100\text{nm}$ ) of ferroelectric polymers of macroscopic lengths are difficult to obtain due to high concentrations needed in solution. Combining ferroelectric and conducting polymers can lead to new functional composite materials in the form of nanofibers that could benefit from the mechanical, electrical and optical properties of the individual components. Using the electrospinning technique we were able to produce true composite nanofibers of PVDF-TrFE/PEDOT-PSSA at surprising low PVDF-TrFE concentrations in dimethylformamide (DMF)[8]. In this paper, we report on the effect of increasing charge on the electrospun composite nanofibers and demonstrate their use in a Schottky diode.

## 2 Experimental details

PVDF-TrFE (75/25) purchased from Kureha, Japan (KF W#2200) was 99.9% pure and was used as received. The polymer molecular weight was 350,000 and was soluble in N,N-Dimethylformamide (DMF). In this work, the following concentrations of PVDF-TrFE in DMF were prepared: 7 wt%, 5 wt% and 3 wt%. For future reference, each of these solutions is designated as part A.

PEDOT-PSSA was purchased from Bayer Corp. (Baytron P) and used as received. This Bayer product has a 1.3wt% of the polymer in water. Prior to use, the PEDOT-PSSA aqueous solution was filtered using a 0.45 $\mu$ m PTFE syringe filter. For future reference, this solution is designated as part B. Figure 1 shows the chemical structures of the two polymers.

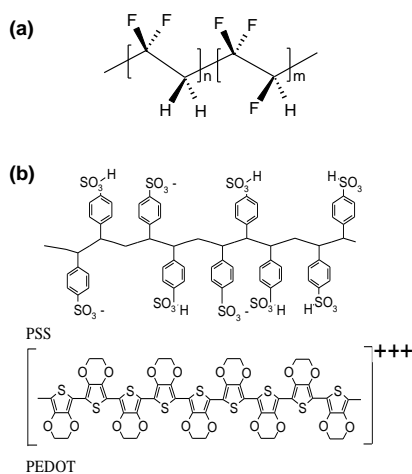


**Figure 1:** Chemical structure of (a) PVDF-TrFE and (b) PEDOT-PSSA

The fibers were prepared by mixing the two solutions above. PEDOT-PSSA was used to increase the charge in the PVDF-TrFE/DMF solution prior to fiber formation. The two parts prepared above were mixed in the following fixed mass ratio for each of the samples studied: 0.85g of part A and 0.037g of part B were mixed slowly in a 20 ml glass vial until the resulting solution was uniform and homogenous with no solid residues-henceforth labeled low charge fibers (LC). For the fiber with increased charge, a larger mass (0.11g) of part B was used, with part A which remained the same-henceforth labeled high charge fibers (HC). Thus for example, a 7wt%-PVDF-TrFE/PEDOT-PSSA (HC) sample for electrospinning was prepared by mixing 0.85g of the 7wt% PVDF-TrFE/DMF solution with 0.11g of the filtered PEDOT-PSSA water solution. The solid polymer PEDOT-PSSA mass to that of PVDF-TrFE was calculated to be 2.3%, 3.2% and 5.3% for the 7wt%-PVDF-TrFE/PEDOT-PSSA, 5wt%-PVDF-TrFE/PEDOT-PSSA and 3wt%-PVDF-TrFE/PEDOT-PSSA solutions, respectively. For LC fibers, the solid polymer PEDOT-PSSA mass to that of PVDF-TrFE was calculated to be 0.81%, 1.13% and 1.89% for the 7wt%-PVDF-TrFE/PEDOT-PSSA, 5wt%-PVDF-TrFE/PEDOT-PSSA and 3wt%-PVDF-TrFE/PEDOT-PSSA solutions, respectively.

The composite nanofibers were prepared via electrospinning using the basic experimental setup shown in Figure 2. About 0.5 ml of the appropriate solution prepared as indicated above was placed in the hypodermic syringe (tuberculin syringe) and the needle connected to the power supply, with the cathode grounded and situated about 20 cm from the tip of the needle. The flow rate was controlled so that a drop fell out from the needle every 20 seconds

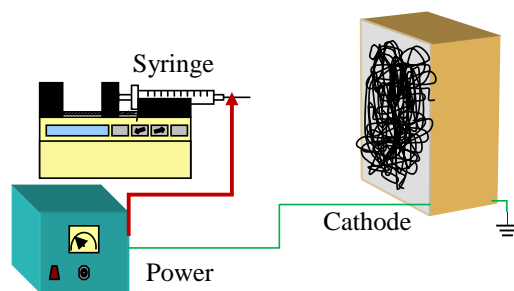


**Figure 2:** Basic electrospinning apparatus

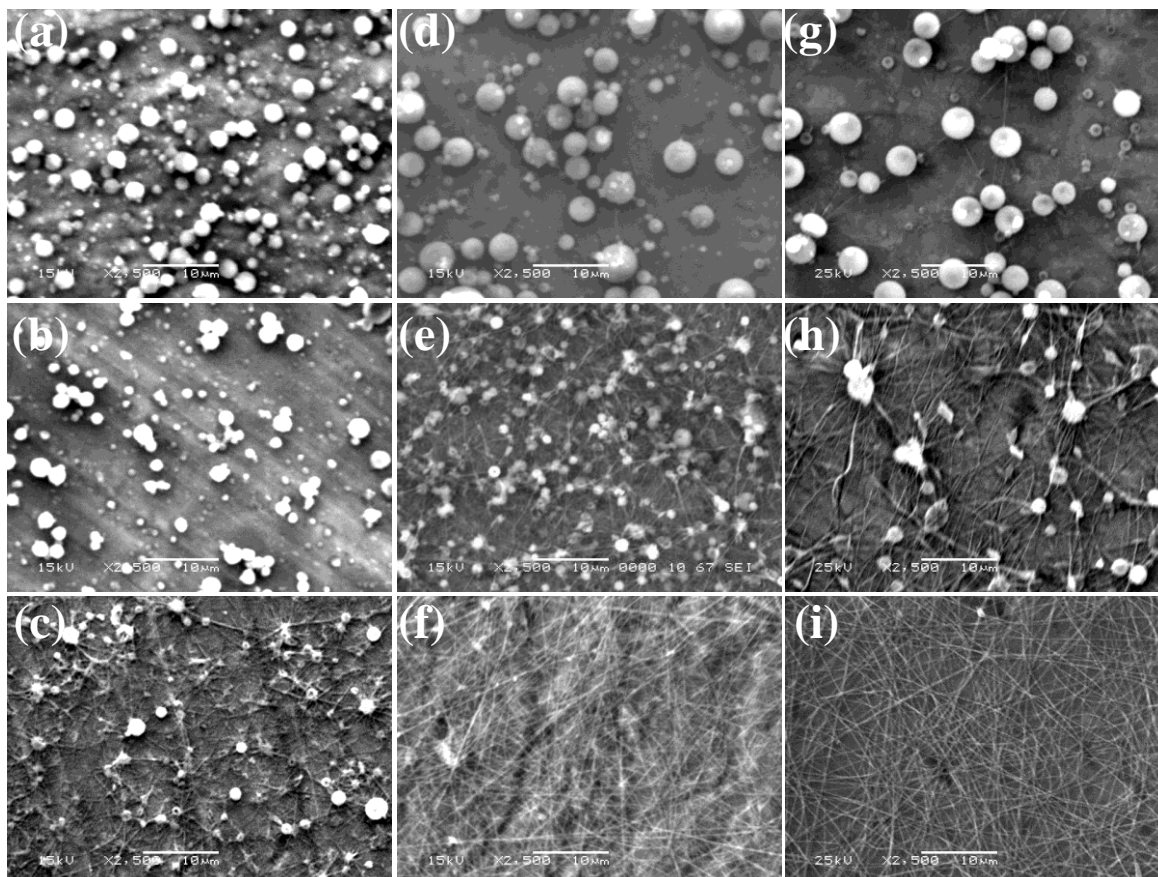
(~2mL/hr). As the voltage applied to the needle increased to about 8-10 kV, the electric force on the polymer droplet at the end of the needle overcomes the surface tension and a jet is issued forth in the form of a very fine spiral. Then, as the solvent evaporates, fibers of the polymer are seen to collect on the cathode (Al foil). Some of the fibers were also captured on pre-patterned *n*-doped Si/SiO<sub>2</sub> substrates to be later tested as Schottky diodes. All fiber samples were annealed in air at 80C for several hours prior to characterization.

### 3 Results and Discussion

Figure 3 shows SEM images of the electrospun solutions prepared above. The SEM images of electrospun pure PVDF-TrFE/DMF solutions without PEDOT-PSSA are shown in Figures 3(a),(d),(g) and for 3, 5 and 7 wt% respectively. Due to low polymer concentration there are no fibers for 3 and 5wt% but mostly beads, but one begins to notice a few isolated fibers bridging the polymer beads for the 7wt% sample (Fig.3(g)). At such low concentrations, the break-up of the electrospun jet due to reduced solution viscosity, combined with the inability of the polymer chains to stay “entangled” once airborne, prevent the formation of fibers as the solvent evaporates. The high boiling point of DMF also necessitates the use of a higher polymer concentration for fiber formation. In essence, what is observed is similar to a spraying effect that covers the cathode with tiny droplets (as a larger portion of the jet is the solvent that requires a longer time to evaporate) and solid beads as was observed on the Al foil after termination of the electrospinning process. A small portion of the polymer deposited on the cathode could therefore have also been from dried liquid drops that lead the formation of thin films/powdery residue inter-dispersed with polymer beads due to electrospinning. Clearly these solutions are not useful in obtaining fibers and need to be modified. One way is to increase the concentration of PVDF-TrFE leading to more viscous solutions, but this leads to thick fibers. Another method of retaining the original viscosity and still obtain fibers is to increase the charge present in the solutions. In the electrospinning process it is known that a net charge density in the electrospinning jet and reduced surface tension lead to uniform fibers without beads. This could be accomplished by using an ionic salt (i.e. NaCl) to the solution[10]. We have chosen to increase the solution charge density by using a conducting polymer PEDOT-PSSA instead. By increasing the amount of conducting polymer there was an increase in the quantity and quality of fibers formed. Figures 3(b),(e),(h) show SEM images for LC fibers. The appearance of fibers is most visible in the 7wt% sample (Fig. 3(h)) although there are still a substantial number of beads present and the fiber lengths are a few microns long. Figures 3(c), (f), (i) shows SEM images for the HC fibers. Clearly we see that PEDOT-PSSA actively assists in the formation of nanofibers without the beading effect as seen for example in Figure 3(i) with typical fiber lengths being several hundreds of microns long, and by being present in the fiber as tested in the device below. The role of the PEDOT-

PSSA in the electrospinning process is therefore multifold: (i) increase the solution charge density (ii) lower the solution surface tension (iii) facilitate the formation of nanofibers from dilute polymer solutions and (iv) retain the conducting properties in the composite nanofibers

**Figure 3:** SEM images of electrospun fibers of (a) 3wt% PVDF-TrFE (b) 3wt% PVDF-TrFE/PEDOT-PSSA



(LC) (c) 3wt% PVDF-TrFE/PEDOT-PSSA (HC); (d) 5wt% PVDF-TrFE (e) 5wt% PVDF-TrFE/PEDOT-PSSA (LC) (f) 5wt% PVDF-TrFE/PEDOT-PSSA (HC); (g) 7wt% PVDF-TrFE (h) 7wt% PVDF-TrFE/PEDOT-PSSA (LC) (i) 7wt% PVDF-TrFE/PEDOT-PSSA (HC). The magnification is the same in all images and the scale bar is 10  $\mu\text{m}$ .

thereby increasing the potential functionality of the nanofiber. The diameters of these fibers measured using a profilometer were in the range 10-30nm. Fibers of such thin dimensions have the potential to lead to new applications where size, sensitivity and a combination of ferroelectric and/or conducting properties are important considerations.

The physical appearance of the fibers were bluish in color, similar to PEDOT-PSSA. While individual fibers had very high resistances ( $> 1\text{G}\Omega$ ), the electrospun fiber mat was conducting and motivated us to fabricate and test Schottky diode. This is a two terminal device and consists of a junction of a *p*-doped polymer with an *n*-doped inorganic semiconductor. The Schottky diode was prepared by using an *n*-doped Si wafer ( $\langle 111 \rangle$ , 0.1-1.0  $\Omega\text{-cm}$ ) with a 200 nm thermally grown oxide layer and 3wt%-PVDF-TrFE/PEDOT-PSSA (HC) fibers. After pre-patterning gold electrodes over the oxide via standard lithography and lift-off techniques, the substrate was cleaved through the electrodes. The exposed cleaved surface has the edge of the gold electrode separated from the doped Si by the insulating oxide layer. The cleaved substrate was then placed on the Al foil during the electrospinning process and covered with nanofibers, many of which were long enough and crossed over the wafer edge making contact

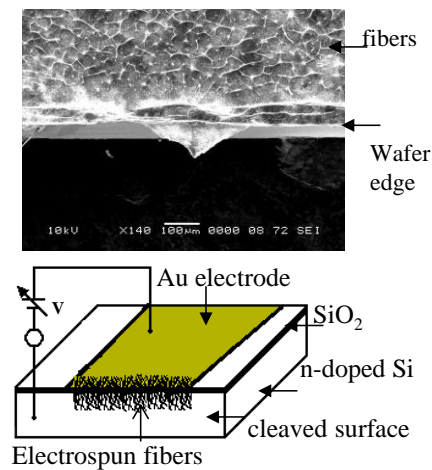


**Figure 4:** Top: SEM image of fibers crossing the wafer edge. Bottom: Schematic of the device with the external electrical connections

to the Au electrode above and to the doped Si below the oxide layer. The resulting Schottky diode was formed along the vertical edge of the cleaved substrate at the nanofibers/*n*-doped Si interface[11]. Figure 4 shows the top view optical image of the device where the cleaved section cuts through a gold electrode and several fibers are seen to reach over the wafer edge. Figure 4 also shows the device schematic with the external electrical connections.

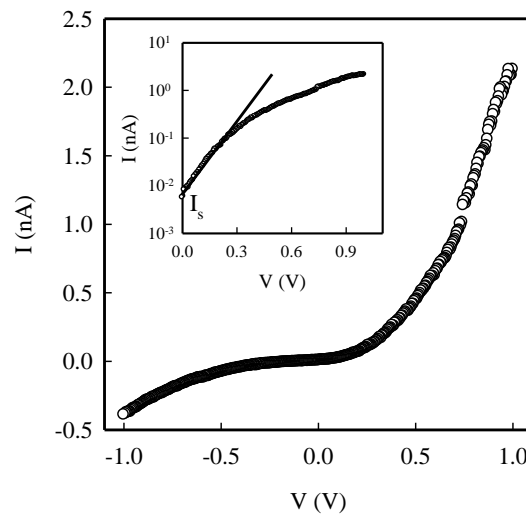


**Figure 5:** I-V characteristic curve for the diode. Inset: Forward bias plot on a semi-log scale. The current intercept at zero  $V$  is the saturation current  $I_s$ .

Figure 5 shows the I-V characteristic curve at 300 K of the device in vacuum. Since the fibers make Ohmic contacts with Au electrodes, the non-linear response arises from Schottky barrier at the polymer-*n*-doped Si substrate. Under thermal equilibrium conditions with no applied external bias to the diode, the Fermi levels of the doped Si and that of PEDOT-PSSA in the fiber mat must coincide leading to band bending at the junction via charge flow from the semiconductor into the polymer. This band bending creates a space charge region resulting in a barrier to charge flow at the interface of the nanofiber and the semiconductor. For typical Schottky diodes, charge flow is via thermionic emission over the barrier and generally, the barrier height is determined by factors such as the polymer work function and the surface

states on the semiconductor[12]. These devices exhibited rectifying behavior and the ratio of the forward to reverse current at a bias voltage of  $\pm 1V$  for this device was calculated to be  $\sim 5$  and was limited in part due to the low fiber conductivity and the series resistance of the bulk semiconductor. The turn-on voltage obtained by extrapolating the current in the linear region ( $V > 0.6V$ ) to the voltage axis at zero current in Figure 5 was  $\sim 0.52V$ .

In order to quantitatively analyze the diode characteristics we assume the standard thermionic emission model of a Schottky junction as follows[13]:

$$J = J_s [\exp(\frac{qV_B}{nkT}) - 1] \quad (1)$$

$$J_s = A^* T^2 \exp(-\frac{q\phi_B}{kT}) \quad (2)$$

where  $J$  is the current density (current/area),  $J_s (=I_s/A)$  is the saturation current density,  $q$  is the electron charge,  $k$  is the Boltzmann constant,  $T$  is the absolute temperature,  $\phi_B$  is the barrier height and  $n$  is the ideality factor which takes into account corrections to the original simple model e.g. image-force barrier lowering. The Richardson's constant ( $A^* = 4\pi q m^* k^2 / h^2$ ) is calculated to be  $120 \text{ A/K}^2\text{-cm}^2$  assuming  $m^*$  is the bare electron mass. Using the data in Figure 5 as an example, the inset to this Figure shows a representative semi-logarithmic plot of the diode current versus applied voltage under forward bias conditions. At low biases a linear variation of the current is observed consistent with Equation (1) while the deviation from linearity at higher bias voltages generally is related to Ohmic losses due to the diode series resistance. Assuming a uniform single layer of 20nm fibers crossing over the edge in Figure 4 and extrapolating the linear portion of the semi-log plot to the current axis at zero bias yields a saturation current density of  $7.2 \times 10^{-5} \text{ A/cm}^2$  and the diode ideality factor calculated from the slope of the linear portion of this plot as follows:

$$n = \frac{q}{kT} \left( \frac{\partial V_B}{\partial \ln J} \right) \quad (3)$$

is  $n \sim 3.2$ . Using these equations we calculate the barrier height of 0.65 eV. The high values ( $n > 1$ ) of the ideality parameter have been attributed to several factors that include the recombination of holes and electrons in the depletion layer, the presence of an interfacial layer and interface states at the polymer-semiconductor interface or even a tunneling process[8]. Since the silicon substrate was not vacuum cleaved, there exists a strong possibility of the presence of dangling Si bonds at the cleaved surface that could interact with the fiber leading to an interfacial layer. Pre-treating the substrates with dilute nitric acid could reduce this effect. Finally, the low turn-on voltage is especially beneficial for polymer based electronics that currently operate under high biases.

#### 4 Conclusions

Composite nanofibers of PVDF-TrFE with PEDOT-PSSA were successfully fabricated via electrospinning. The addition of PEDOT-PSSA increases the charge in solution and assists in fiber formation making it possible to electrospin uniform nanofibers of PVDF-TrFE at low polymer concentrations in DMF and without the beading effect in PVDF-TrFE solutions with high polymer concentrations. The incorporation of PEDOT-PSSA into the nanofibers was verified via fabricating and testing a Schottky diode. The electrospinning process for generating nanofibers is economical and simple to operate. Nanofibers of PVDF-

TrFE/PEDOT-PSSA are promising candidates for use in a variety of applications that require the ferroelectric and/or conducting properties of the composite fibers. In addition, the large aspect ratio and even larger surface to volume ratio of the fibers makes them ideal candidates in the fabrication of miniaturized, low power consumption devices and supersensitive sensors.

**Acknowledgement:** This work was supported in part by NSFDMR under grants RUI-0965023 and PREM-0934195 and by DoD under grant W911NF-11-1-0184.

## References

- [1] Chiang C.K., Fincher Jr. C.R., Park Y.W., Heeger A.J., Shirakawa H., Louis E.J., Gau S.C., MacDiarmid A.G., Electrical conductivity in doped polyacetylene, *Phys. Rev. Lett.* **39**, 1098-1101 (1977).
- [2] Chiang J.C., MacDiarmid A.G., Polyaniline: Protonic acid doping of the emeraldine form to the metallic regime, *Synth. Metals* **13**, 193-205 (1986).
- [3] Yamada T., Kitayama T., Ferroelectric properties of vinylidene fluoride-trifluoroethylene copolymers, *J. Appl. Phys.* **52**, 6859-6863 (1981).
- [4] Lovinger A.J., Furukawa T., Davis G.T., Broadhurst M.G., Crystallographic changes characterizing the Curie transition in three ferroelectric copolymers of vinylidene fluoride and trifluoroethylene: 1. As-crystallized samples, *Polymer* **24**, 1225-1232 (1983).
- [5] Koizumi N., Haikawa N., Habuka H., *Ferroelectrics* **57**, 99-102 (1984).
- [6] Reece T.J., Ducharme S., Sorokin A.V., Poulsen M., Nonvolatile memory element based on a ferroelectric polymer Langmuir–Blodgett film, *Appl. Phys. Lett.* **82**, 142-144 (2003).
- [7] Park Y.J., Kang S.J., Lotz B., Brinkmann M., Thierry A., Kim K.J., Park C., Ordered Ferroelectric PVDF–TrFE Thin Films by High Throughput Epitaxy for Nonvolatile Polymer Memory, *Macromolecules* **41**, 8648-8654 (2008).
- [8] Martinez O., Bravo A.G., Pinto N.J., Fabrication of poly(vinylidene fluoride-trifluoroethylene)-poly(3,4-ethylenedioxythiophene) polystyrene sulfonate composite nanofibers via electrospinning, *Macromolecules* **42**, 7924-7929 (2009).
- [9] Abreu M., Montañez S., Pinto N.J., Electrospun composite nanofibers of poly(vinylidene fluoride-trifluoroethylene)/polyaniline-polystyrene sulfonic acid, *J. Appl. Poly. Sci.* **119**, 3640-3644 (2011).
- [10] Fong H., Chun I., Reneker D.H., Beaded nanofibers formed during electrospinning, *Polymer* **40**, 4585-4592 (1999).
- [11] Pinto N.J., Johnson A.T., MacDiarmid A.G., Muller C.H., Theofylaktos N., Robinson D.C., Miranda F.A., Electrospun polyaniline/polyethylene oxide nanofiber field-effect transistor, *Appl. Phys. Lett.* **83**, 4244-4246 (2003).
- [12] Sze S.M. *Physics of Semiconductor Devices*, John Wiley & Sons, New York (1981).
- [13] Horowitz G., Organic Semiconductors for new electronic devices, *Adv. Mater.* **2**, 287-292, (1990).